

Abrasive Flow Machining for Enhancing Surface Quality of 3D-Printed Millimeter-Wave Waveguides

Lu Qian⁽¹⁾, Sean Trengove⁽²⁾, Nathan Miller⁽³⁾, Talal Skaik⁽¹⁾, Yi Wang⁽¹⁾

⁽¹⁾ School of Engineering, University of Birmingham, United Kingdom
Email: {l.qian.1; t.f.skaik; y.wang.1}@bham.ac.uk

⁽²⁾ Extrude Hone Ltd, Sovereign Business Park, Milton Keynes MK8 0JP, United Kingdom
Email: Sean.Trengove@extrudehone.com

⁽³⁾ Flann Microwave Ltd, Dunmere Rd, Bodmin PL31 2QL, United Kingdom
Email: nathan.miller@flann.com

ABSTRACT

Poor surface quality is a well-known challenge in additively manufactured monolithic waveguide components, particularly as the frequency extends into the mm-wave spectrum. To address this issue, a polishing method based on abrasive flow machining (AFM) is investigated. It applies abrasive media to polish difficult-to-access internal surfaces and effectively reduces the surface roughness. This work demonstrates the application of AFM technique to two sets of mm-wave waveguide twists for WR-15 (50–75 GHz) and WR-5 (140–220 GHz) bands in an end-to-end process – printing, polishing and plating. The twist waveguides were fabricated using high-precision micro laser sintering (MLS) technology. Measurements were performed before and after the AFM polishing. The impact of polishing on both mechanical (dimensional accuracy and surface characterization) and electrical (attenuation and return loss) properties was evaluated. Polishing resulted in 70% reduction in surface roughness for all waveguide twists, achieving submicron roughness levels ($<1\ \mu\text{m}$). The material removal rate was averaged $200\ \mu\text{m}$. For the WR-15 twist, the dissipative attenuation factor was reduced from 5.4 to 3 dB/m, with a worst-case return loss of 30 dB. Similarly, for the WR-05 twist, the attenuation factor decreased from 16 to 10 dB/m, with a worst-case return loss of 14 dB. This study establishes the feasibility of using AFM for polishing the internal surfaces of 3D-printed mm-wave waveguides.

INTRODUCTION

The low loss characteristics of air-filled metallic waveguide (WG) make this technology a preferred solution for many passive devices in space applications over the millimeter-wave (mm-wave) bands, where dissipative attenuation of the signal is a critical detrimental factor. However, the manufacturing complexity and cost present significant challenges to the widespread usage of WGs in these spectra. Compared to waveguide operating in the microwave spectrum, mm-wave WG components have much smaller feature sizes and require higher surface finishing quality.

Traditionally, these WG structures are manufactured through machining such as computerized numerical control (CNC) milling or electrical discharge machining (EDM), or by reshaping metal pipes through rectangular dies [1], [2]. As frequency increases into the mm-wave band, the manufacturing cost rises due to the need for greater precision for smaller feature sizes. More recently, metal additive manufacturing (AM, also known as 3D printing), particularly Laser Powder Bed Fusion (L-PBF), has emerged as a new fabrication method for WG components, due to its unparalleled capability for rapid prototyping and its flexibility in creating monolithic structures with complex geometries. It is important to note that 3D-printed metal components exhibit superior mechanical and thermal properties to their polymer counterparts. Many microwave components have been reported [3], [4], [5], [6], using 3D printers with manufacturing tolerances on the order of 100–150 μm . With the increased availability of higher-precision 3D printers (offering tolerance down to 5–10 μm), a number of mm-wave WG devices have also been developed [7], [8], [9], [10], [11], [12], [13]. However, one of the major challenges with 3D-printed metallic WG components is their inferior surface quality compared to conventional subtractive manufacturing. High surface roughness not only increases conductor losses but also degrades electro-thermal performance [14]. To improve surface quality, ceramic particles were used in a vibratory grinding machine to improve the surface quality of a 3D-printed Invar filter [6]. More recently, a low-cost, barrel-based surface polishing method was reported [15], where a rotary tumbler was used with 300–400 μm microbeads, resulting in an 18% reduction in surface roughness. However, these conventional mechanical treatments are limited by the size of the polishing media. At mm-wave and sub-THz frequencies, the reduced cross-sectional dimensions of long channels or cavities make it increasingly difficult, if possible at all, to reach internal areas for polishing.

In this work, we investigated the use of Abrasive Flow Machining (AFM) for the internal surface treatment of monolithically 3D-printed, irregular shaped, mm-wave waveguides in the form a twist, aiming to reduce the internal surface roughness. AFM has been used to post process complex metal passages for gas flow, fuel injection systems, rocket propulsion pumps and rotating parts in jet engines. It is also used to process 3D printed hydraulic manifolds to ensure any partially sintered particles are removed to eliminate the risk of catastrophic failure. To the best of the authors' knowledge, this work is the first demonstration of AFM in mm-wave waveguide devices in the open literature.



Fig. 1. Photographs of the mm-wave twist waveguides: (a) As-printed waveguide twist sections; (b) Assembled with the flanges and after AFM polishing and after gold plating.

3-D PRINTED MONOLITHIC WAVEGUIDE TWISTS

The experimental study was conducted on WR-15 (50–75 GHz) and WR-5 (140–220 GHz) waveguide twists. Twists at these bands are non-trivial waveguide structures typically used for interconnections. Shown in Fig. 1 are the devices under test formed of a twist and a bent structure and two standard UG-387 flanges. The flanges are machined separately and brazed onto the 3D printed waveguide sections in this case. The cross-section of the twists is the standard WR-15 and WR-05 waveguides, while the length is 35 mm. The bent-twist structure was chosen to verify the net-shaping capability of the 3D printing and the AFM surface treatment technique.

A DMP60 series printer from 3D MicroPrint, utilizing high-precision micro laser sintering (MLS) technology, was employed. The samples were printed in one batch, with three for each type to verify reproducibility. To ensure monolithic printing without overhang structures, the waveguide sections were tilted at 45° during printing. External support structures were used. The wall thickness for all samples was 0.5 mm. The printing material was stainless steel 1.4542 (17-4PH). The nominal manufacturing tolerance and surface roughness is 5-10 μm and 3-5 μm , respectively. Fig. 1(a) shows the as-printed waveguide samples.

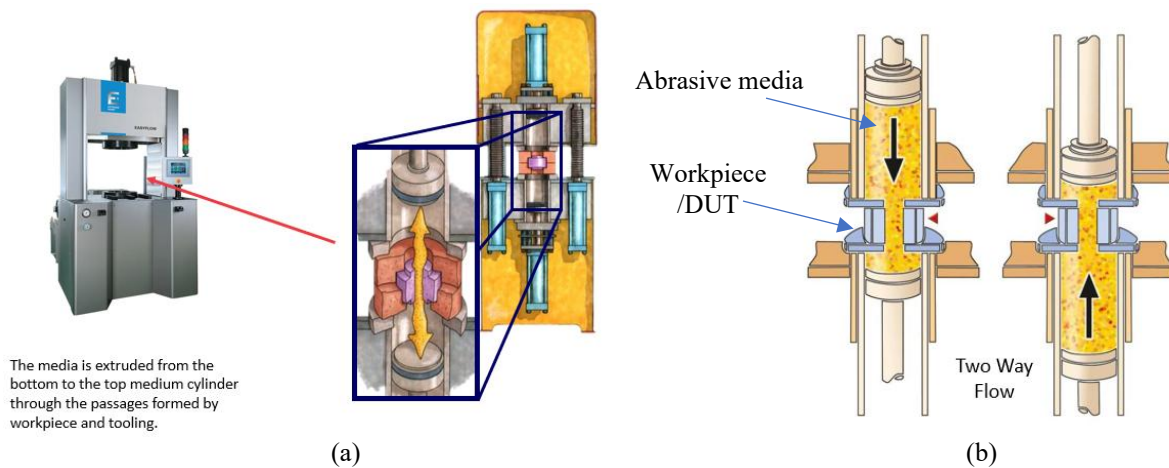


Fig. 2. Schematic illustration of (a) the Extrude Hone machine and (b) the two-way AFM process.

ABRASIVE FLOW MACHINING (AFM)

Polishing the internal surfaces of these long, narrow waveguide channels in these twists is the most challenging aspect of the end-to-end process. The use of Extrude Hone AFM was experimented. The AFM is a finishing process developed to machine difficult-to-reach internal surfaces. Abrasive media are extruded under pressure through or across the target surface to achieve the desired finish. Fig. 2 provides a schematic illustration of the machine and the process. Common

AFM methods are classified into four types [16]: (1) One-way AFM, (2) Two-way AFM, (3) Multi-way AFM, and (4) Orbital AFM. A preliminary trial of a one-way AFM process on the internal surface of a waveguide was reported in [17]. In our work, a two-way process is used. Compared to the one-way process, it provides more uniform finishing and achieves tighter tolerances. A chemically inactive and non-corrosive medium (polyborosiloxanes) is utilized.

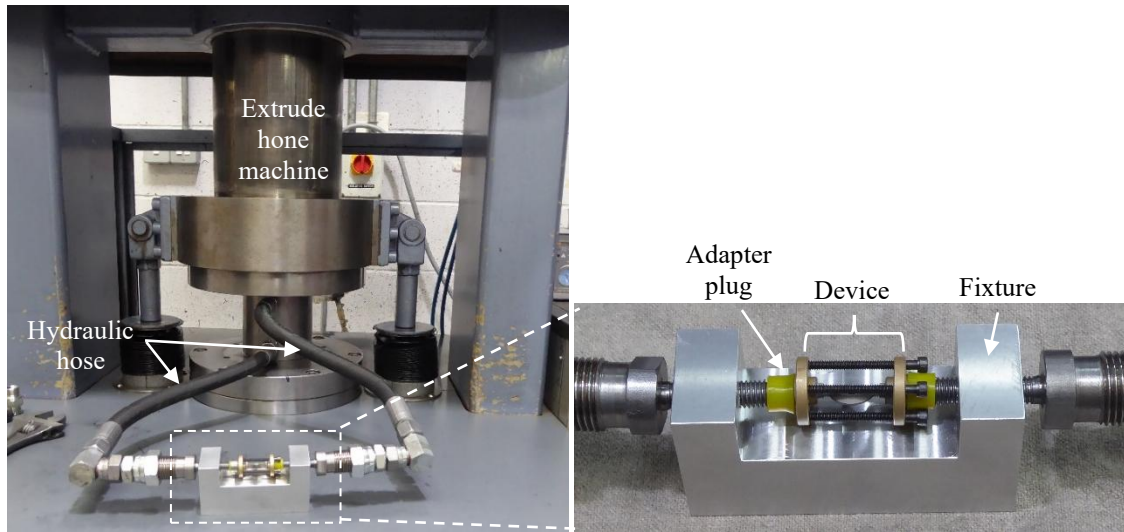


Fig. 3. Extrude Hone AFM setup for the waveguide device when the process is done outside the machine with hoses.

The AFM setup is shown in Fig. 3. The abrasive media is pumped from the extrude hone machine through a hydraulic hose to the fixture clamping the waveguide device. Another hose takes the media back to the machine and then the flow reverses. Two soft adapter plugs (yellow) are used to feed the abrasive media into the waveguide. To fully protect the ends of the waveguide from erosion at the entrance and exit, the plugs could be replaced with metal end plates. The process is fully automatic. The flow of the abrasive media is controlled with precise hydraulic servo valves in closed loop feedback. The advanced controls allow to control volumetric flow rate, total volume, pressure, and temperature in various modes and combinations. All metal material can be processed by selecting abrasive of the appropriate hardness. The smallest processable holes can be down to 50 μm if the length-diameter ratio is less than 10:1.

GOLD PLATING

After polishing, both waveguide twists were gold-plated using an electroless process[13]. It comprises the following steps: rinse, degreasing soak, rinse, acid dip, rinse, Wood's nickel strike, electroless nickel plating, and immersion/autocatalytic gold plating. A peristaltic pump was used to move the plating solutions along the internal channel of the twists. Fig. 1(c) shows the gold-plated waveguide twists.

EXPERIMENTAL RESULTS

First, the mechanical properties (including dimensions and surface roughness) of the waveguide twists were assessed using an Alicona G4 InfiniteFocus Optical system. Table 1 summarizes the measured dimensions and surface roughness before and after AFM process. The surface roughness of the as-printed samples is around 2.5 μm . After AFM, a nearly 70% reduction was achieved, reducing the surface roughness to below 1 μm . This is a significant reduction.

Table 1 Mechanical Properties of Fabricated Prototypes

	Waveguide	Design	As-Printed	AFM
Port Dimension $a \times b$ (mm)	WR15	3.76 \times 1.88	3.72 \times 1.87	3.92 \times 2.15
	WR05	1.30 \times 0.65	1.27 \times 0.65	1.43 \times 0.85
Surface Roughness (μm)	WR15	-	2.56	0.82
	WR05	-	2.48	0.73

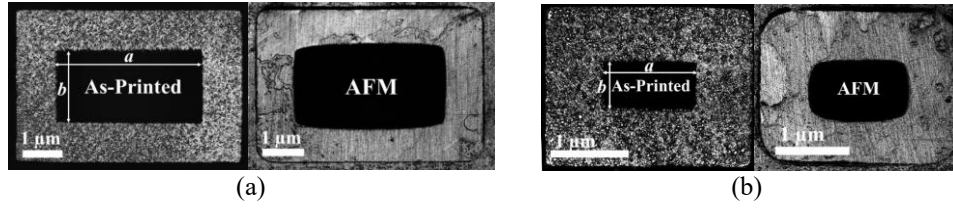


Fig. 4. Waveguide cross sections, as printed and after AFM polishing processes: (a) WR-15 twists. (b) WR-05 twists.

An observation from Fig. 4 is the impact of the AFM treatments on the cross-sectional shape of the waveguide. The rounding effect is clear. This is expected from the medium-based AFM process. As shown in Table 1, the dimensional deviation introduced by the AFM is approximately $210\ \mu\text{m}$. These are first-shot results without any pre-compensation. In practical production, these deviations in the geometry and dimensions can be mitigated through pre-design adjustments.

RF measurements were performed using a Keysight N53478B PNA-X network analyser. Fig. 5 shows the simulated and measured frequency responses. In the simulations, the conductivity was set to represent ideal smooth stainless steel and gold. It is clear that a significant reduction in insertion loss (IL) was achieved after AFM, although some degradation in the in-band matching was observed.

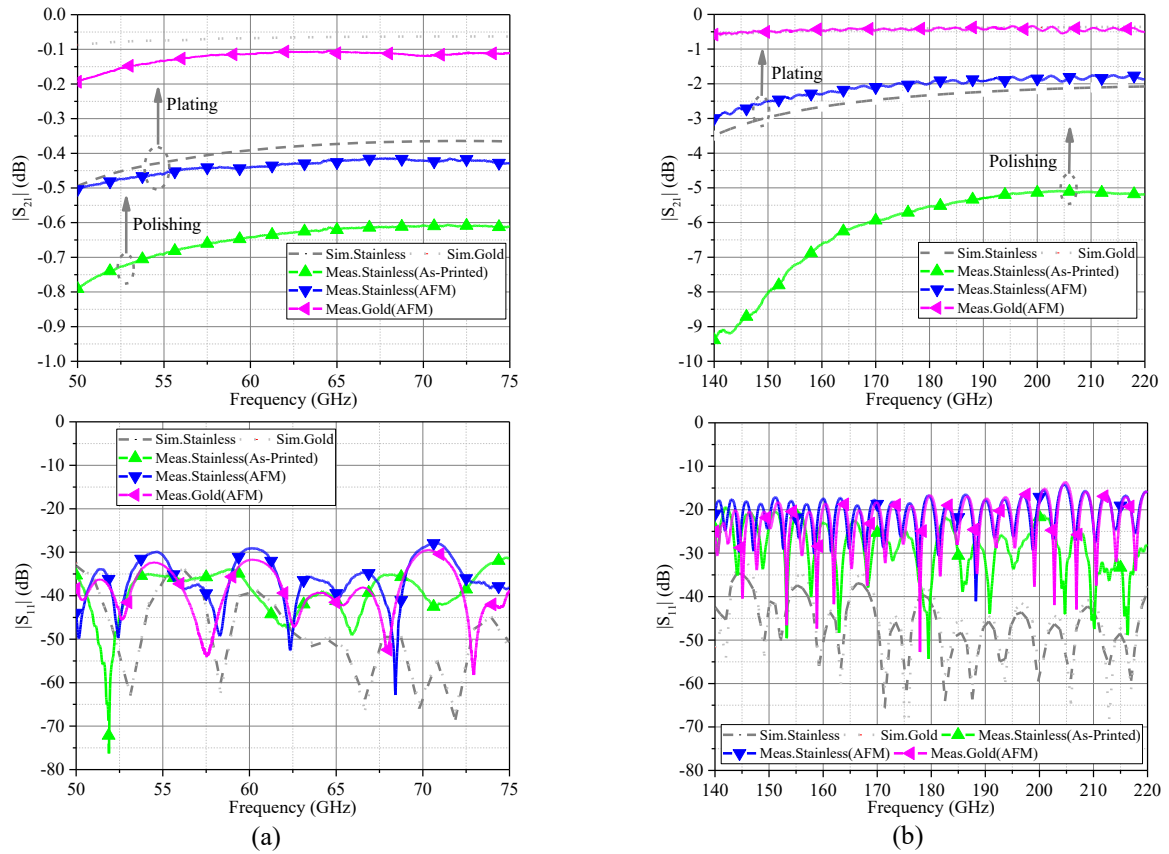


Fig. 5. Measurement results in comparison with simulations before and after AFM as well as gold plating: (a) WR15; (b) WR05

For the WR-15 twist, the measured return losses in Fig. 5(a) are over 30 dB across the band. As expected, the stainless-steel twist after AFM polishing has higher reflection due to the change of waveguide cross-section. As mentioned earlier, pre-compensation should improve this. The IL was reduced from 0.65 dB to 0.45 dB, which is very close to the simulated 0.40 dB for ideal stainless steel. After gold plating, the measured IL was further reduced to 0.12 dB (AFM). This is very close to the ideal 0.07 dB insertion loss for gold. The significant reduction in insertion losses demonstrates the effectiveness of the AFM process.

For the WR-05 twist, a 20-dB difference between the simulated and measured $|S_{11}|$ was observed after the AFM treatment as shown in Fig. 5(b). This large return loss degradation is again due to the dimensional changes. The $|S_{11}|$ remains below

-10 dB across the band. A more impressive improvement was observed in the $|S_{21}|$. The achieved insertion loss after gold plating was 0.44 dB after AFM, close to the predicted 0.43 dB for gold. These improvements again show the effectiveness of the polishing method.

CONCLUSION

This paper demonstrates an end-to-end AM-based fabrication solution for millimeter-wave waveguide devices. This includes a high-precision MLS printing technology, an AFM based surface polishing method, and an electroless gold plating technique. Dimension metrology shows good printing quality and repeatability. Experimental results confirm that the AFM process effectively reduce the surface roughness from 2.5 μm to below 1 μm . This correlates well with the improvement seen in the measured IL after polishing. Some degradation in return loss was introduced by polishing due to the removal of materials, which was not pre-compensated in the design, and therefore change of the cross-sectional geometry. This study demonstrates the effectiveness of the proposed end-to-end fabrication solution in manufacturing small, enclosed monolithic waveguide structures, with performance potentially comparable to traditional (micro)machining methods. The AFM process is expected to be applicable to most uniform waveguide structures. Its impact on geometry, due to material removal, however, should be carefully considered and pre-compensated in the design.

REFERENCES

- [1] P. J. Chou and R. Siemann, "Measurements of losses in EDMed waveguides and in first W-band structure," *ARDB Tech. Note*, vol. 99, 1997.
- [2] I. Stil, A. L. Fontana, B. Lefranc, A. Navarrini, P. Serres, and K. F. Schuster, "Loss of WR10 waveguide across 70–116 GHz," in *Proc. 22nd Int. Symp. Space Terahertz Technol*, National Radio Astronomy Observatory, 2012, pp. 1–3.
- [3] O. A. Peverini, M. Lumia, G. Addamo, G. Virone, and N. J. G. Fonseca, "How 3D-Printing Is Changing RF Front-End Design for Space Applications," *IEEE Journal of Microwaves*, vol. 3, no. 2, pp. 1–15, Apr. 2023, doi: 10.1109/jmw.2023.3250343.
- [4] P. Booth and E. V. Lluch, "Enhancing the Performance of Waveguide Filters Using Additive Manufacturing," *Proceedings of the IEEE*, vol. 105, no. 4, pp. 613–619, Nov. 2016, doi: 10.1109/jproc.2016.2616494.
- [5] L. Qian, R. Martinez, M. Salek, T. Skaik, M. Attallah, and Y. Wang, "Compact Monolithic 3D-Printed Wideband Filters Using Pole-Generating Resonant Irises," *IEEE Journal of Microwaves*, vol. 3, no. 3, pp. 1028–1039, Jul. 2023, doi: 10.1109/JMW.2023.3271433.
- [6] L. Qian *et al.*, "A Narrowband 3-D Printed Invar Spherical Dual-Mode Filter With High Thermal Stability for OMUXs," *IEEE Trans Microw Theory Tech*, vol. 70, no. 4, pp. 2165–2173, Apr. 2022, doi: 10.1109/TMTT.2022.3152795.
- [7] M. Salek *et al.*, "W-Band Waveguide Bandpass Filters Fabricated by Micro Laser Sintering," *IEEE Transactions on Circuits and Systems II: Express Briefs*, vol. 66, no. 1, pp. 61–65, 2019, doi: 10.1109/TCSII.2018.2824898.
- [8] Y. Yu *et al.*, "D-Band Waveguide Diplexer Fabricated Using Micro Laser Sintering," *IEEE Trans Compon Packaging Manuf Technol*, vol. 12, no. 9, pp. 1446–1457, 2022, doi: 10.1109/TCPMT.2022.3204887.
- [9] K. Van Caekenberghe, P. Bleys, T. Craeghs, M. Pelk, and S. Van Bael, "A W-band waveguide fabricated using selective laser melting," *Microw Opt Technol Lett*, vol. 54, no. 11, pp. 2572–2575, Nov. 2012, doi: 10.1002/mop.27121.
- [10] B. Zhang and H. Zirath, "Metallic 3-D Printed Rectangular Waveguides for Millimeter-Wave Applications," *IEEE Trans Compon Packaging Manuf Technol*, vol. 6, no. 5, pp. 796–804, May 2016, doi: 10.1109/TCPMT.2016.2550483.
- [11] V. Fiorese *et al.*, "Evaluation of Micro Laser Sintering Metal 3D-Printing Technology for the Development of Waveguide Passive Devices up to 325 GHz," in *2020 IEEE/MTT-S International Microwave Symposium (IMS)*, IEEE, Aug. 2020, pp. 1168–1171. doi: 10.1109/IMS30576.2020.9224102.
- [12] T. Skaik *et al.*, "Evaluation of 3-D Printed Monolithic G-Band Waveguide Components," *IEEE Trans Compon Packaging Manuf Technol*, vol. 13, no. 2, pp. 240–248, Feb. 2023, doi: 10.1109/TCPMT.2023.3243002.
- [13] T. Skaik *et al.*, "A 3-D Printed 300 GHz Waveguide Cavity Filter by Micro Laser Sintering," *IEEE Trans Terahertz Sci Technol*, vol. 12, no. 3, pp. 274–281, May 2022, doi: 10.1109/TTHZ.2022.3147042.
- [14] Q. M. Khan and D. Kuylenstierna, "Electro-Thermal Modeling of AM-SLM Based Cavity Resonators," in *2024 IEEE/MTT-S International Microwave Symposium - IMS 2024*, IEEE, Jun. 2024, pp. 505–508. doi: 10.1109/IMS40175.2024.10600376.
- [15] J. Sorocki *et al.*, "Low-Cost Method for Internal Surface Roughness Reduction of Additively Manufactured All-Metal Waveguide Components," *IEEE Trans Microw Theory Tech*, 2024, doi: 10.1109/TMTT.2024.3361976.
- [16] N. Dixit, V. Sharma, and P. Kumar, "Research trends in abrasive flow machining: A systematic review," *J Manuf Process*, vol. 64, no. March, pp. 1434–1461, 2021, doi: 10.1016/j.jmapro.2021.03.009.

- [17] P. A. Ivanov, V. A. Levko, M. M. Mikhnev, and E. V. Patraev, "Abrasive Flow Machining of the Internal Surfaces of 3D-Printed Curved Rectangular Waveguides," *Russian Engineering Research*, vol. 43, no. 9, pp. 1106–1111, Sep. 2023, doi: 10.3103/S1068798X23090113.